J Mater Sci (2010) 45:6266–6270
DOI 10.1007/s10853-010-4822-8

LETTER

Improvement of fracture properties of hydroxyapatite particle filled poly(L-lactide)/poly(ε-caprolactone) biocomposites using lysine tri-isocyanate

Tetsuo Takayama · Mitsugu Todo

Received: 7 June 2010 / Accepted: 10 August 2010 / Published online: 21 August 2010

Abstract Effects of LTI addition on the mode I fracture energy of HA/PLLA/PCL were examined and the microstructural modification due to LTI addition was investigated. Both the mode I energy release rate, G_{in}, and averaged fracture energy, E_f, are improved dramatically due to LTI addition. The reason is considered to be the improvements of the interfacial structure connecting HA particles with PLLA/PCL matrix and the miscibility between PLLA and PCL. These changes of blend morphology and interfacial structure reduce the stress concentration and lead to the ductile deformation and resulted in the increase of those fracture properties.

Poly(L-lactide) (PLLA) is known to be a bioabsorbable polymer with biocompatibility and therefore has widely been used for bone fixation devices in orthopedics and oral surgery [1, 2]. Blending with bioactive ceramics such as hydroxyapatite (HA) has recently been adopted to improve the bioactivity, the degradation rate, and the stiffness of such medical devices [3–15]. It was, however, shown that the fracture properties of such HA/PLLA biocomposites tend to be much lower than those of neat PLLA mainly due to immediate failure along the interfaces between HA particles and PLLA matrix, as a result, brittle fracture behavior is observed in this biocomposite system [16–18]. Park et al. has succeed to improve the ductility of HA/PLLA by blending Poly (ε-caprolactone) (PCL), which is the ductile biocompatible polymer [19]. However, it was also found that the phase separation in PLLA/PCL polymer blend tend to disturb the improvement of fracture toughness. Recently, our research group has discovered that lysine tri-isocyanate (LTI) effectively improves such phase separation, and the fracture toughness of PLLA/PCL is dramatically increased due to LTI addition [20–22]. The aim of the present study was therefore to assess the effect of LTI addition on the fracture properties of HA/PLLA/PCL biocomposites. Microstructural modification by LTI addition was also correlated with the improvement of the fracture properties.

HA particles (Sangi Co., Ltd.) with the representative size of about 5 μm were used as filler. HA particles and PLLA (Toyota Motor Co., Ltd.) and PCL pellets (CelgreenH7® Daicel Chemistry Industries Co.) were mixed by a conventional melt-mixer at 190 °C. LTI was blended with HA particles and PLLA and PCL pellets prior to the melt-mixing. The mixing ratio of HA, PLLA, and PCL was fixed at 10:90:10 in weight fraction, and LTI content was chosen to be 1 wt% to the weight of PLLA/PCL. HA/PLLA/PCL and HA/PLLA/PCL/LTI are denoted thereafter as H/L/C, and H/L/C/T, respectively. For comparison, HA/PLLA composite, denoted as HA/PLLA, and neat PLLA were also prepared by using the same fabrication process. Plates of 2-mm thick were then fabricated from those mixtures using a hot-press attached with a water-cooling system. The mixtures were melted at 180 °C and pressed at 30 MPa, and then quenched to room temperature using the cooling system. Single-edge-notch-bend (SENB) specimens were prepared from the composite plates for mode I fracture testing. The length and width of SENB specimen is 70 and 10 mm, respectively, and the initial notch length is 5 mm. The crystallinity values of PLLA, $x_{c,PLLA}$, were measured using a differential scanning calorimetry.

T. Takayama (✉)
Graduate School of Science and Engineering,
Yamagata University, Yonezawa, Yamagata 992-8510, Japan
e-mail: t-taka@yz.yamagata-u.ac.jp

M. Todo
Research Institute for Applied Mechanics, Kyushu University,
Kasuga, Fukuoka 816-8580, Japan

Three-point bending tests of the SENB specimens were conducted at a loading rate of 1 mm/min, and the mode I energy release rate, G_{in}, at crack initiation was evaluated using the following formula [23]:

$$G_{in} = \frac{U_{in}}{BW\phi} \tag{1}$$

$$\phi = \frac{A + 18.64}{dA/dx} \tag{2}$$

$$A = \frac{16x^2}{(1-x)^2}(8.9 - 33.717x + 79.616x^2 - 112.952x^3 + 84.815x^4 - 25.672x^5) \tag{3}$$

$$dA/dx = \frac{16x^2}{(1-x)^2}(-33.717 + 159.232x - 338.856x^2 + 339.26x^3 - 128.36x^4) + 16(8.9 - 33.717x + 79.616x^2 - 112.952x^3 + 84.815x^4 - 25.672x^5)\left\{\frac{2x(1-x)+2x^2}{(1-x)^3}\right\}, \tag{4}$$

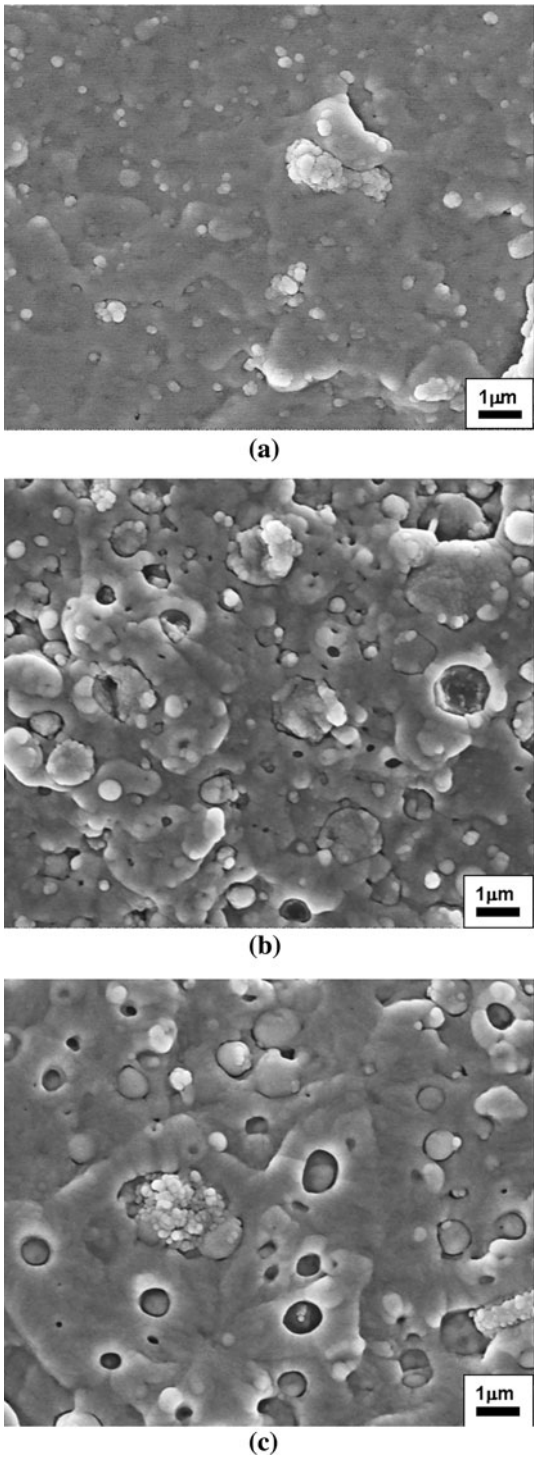

Fig. 1 FE-SEM micrographs of cryo-fracture surfaces. **a** HA/PLLA, **b** HA/PLLA/PCL, and **c** HA/PLLA/PCL/LTI

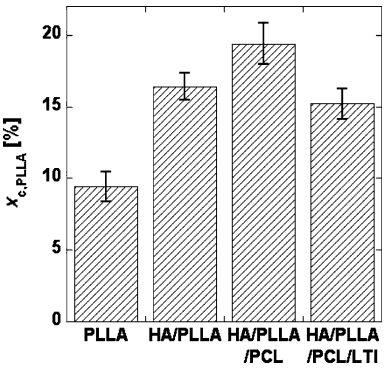

Fig. 2 Effect of LTI on the crystallinity of PLLA, $x_{c,PLLA}$

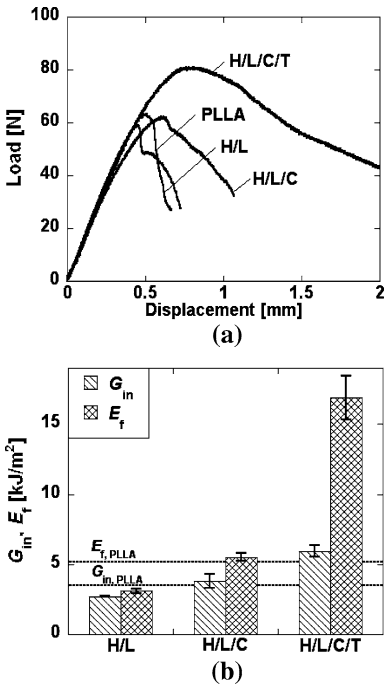

Fig. 3 Results obtained from mode I fracture tests. **a** Typical load–displacement curves and **b** fracture properties

where B, W, and a are the thickness, width, and the initial crack length of the SENB specimen, respectively, and ϕ is the geometrical correction factor given as a function of x that is equal to a/W. U_{in} is the critical energy defined as the area under the load–displacement curve up to the crack initiation point at which the rigidity of the SENB specimen decreased rapidly. The average fracture energy, E_f, was also evaluated and simply defined by the following formula:

$$E_f = \frac{U_f}{W(B-a)}, \quad (5)$$

where U_f is the energy corresponding to the area under load–displacement curve up to the point of complete fracture of the specimen. E_f is therefore recognized as the average fracture energy per unit area of fracture surface. Fracture surface and interface structure between HA particle and matrix of the SENB specimens were also observed using a scanning electron microscope (SEM) and a field emission scanning electron microscope (FE-SEM), respectively.

FE-SEM micrographs of cryo-fracture surfaces of the specimens are shown in Fig. 1. It is noted that the number of spherical PCL decreases due to LTI addition, corresponding to the improvement of the miscibility of PLLA and PCL. This implies that the miscibility of PLLA and PCL is improved by crosslinking of PLLA and PCL macromolecules induced by the chemical reaction between

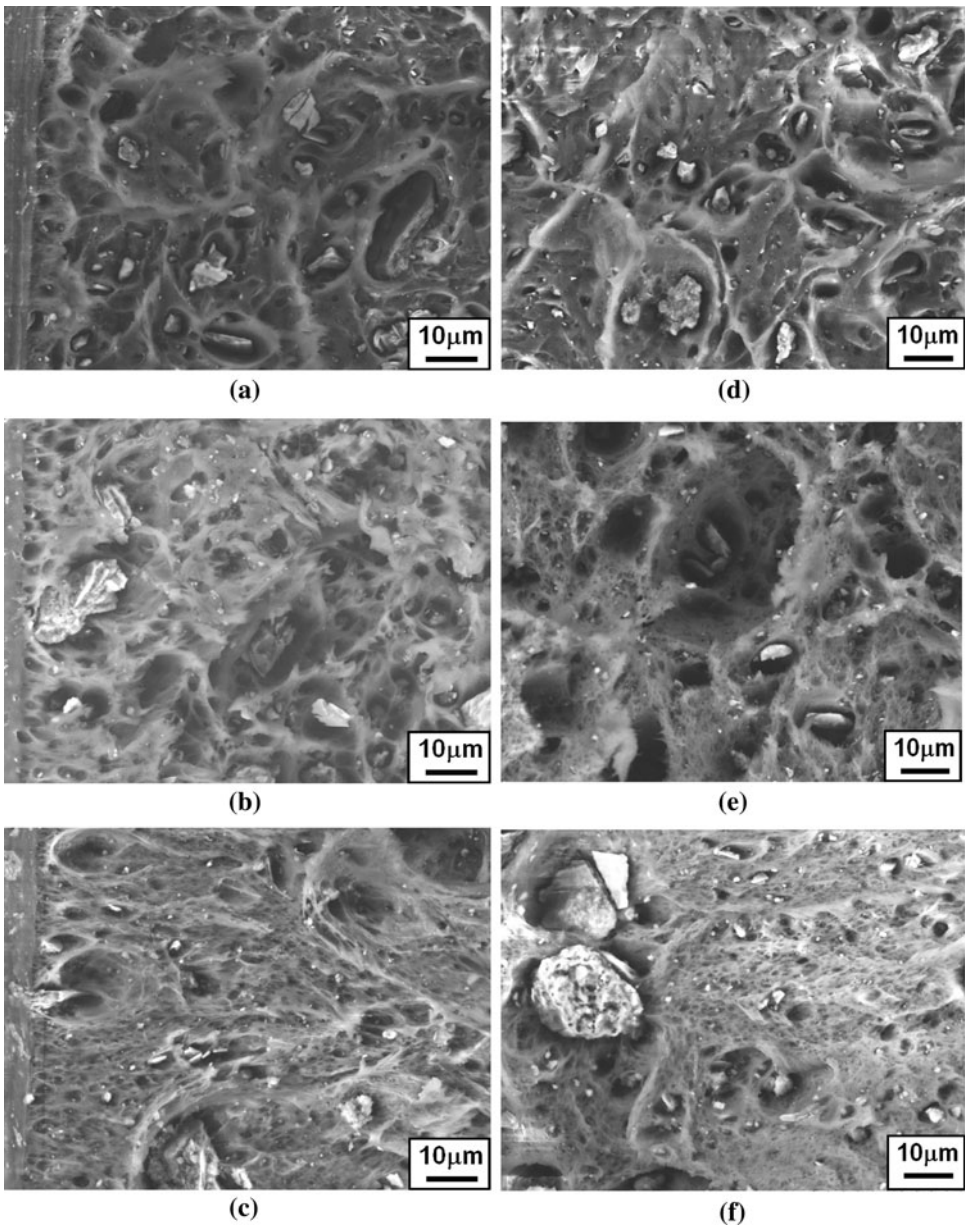

Fig. 4 SEM micrographs of fracture surfaces. **a** HA/PLLA-notch-tip, **b** HA/PLLA/PCL-notch-tip, **c** HA/PLLA/PCL/LTI-notch-tip, **d** HA/PLLA-crack propagation, **e** HA/PLLA/PCL-crack propagation, and **f** HA/PLLA/PCL/LTI-crack propagation

the hydroxyl group of PLLA and PCL and the isocyanate group of LTI [20]. The crystallinity of PLLA, $x_{c,PLLA}$ are shown in Fig. 2. It was found that $x_{c,PLLA}$ tends to increase by PCL blending. It is thought that the crystallization of PLLA is encouraged under existence of PCL spherulites which may work as nuclei [24]. It is interesting to see that the crystallinity of H/L/C/T is lower than that of H/L/C, indicating that such nucleating effect of PCL is reduced because the formation of PCL spherulites is suppressed due to the improvement of the miscibility of PLLA and PCL.

Typical load–displacement curves obtained from the mode I fracture tests are shown in Fig. 3a. It is seen that addition of HA particles degrades the maximum load of PLLA, however, further blending of PCL increases the maximum load. It should be noted that addition of LTI dramatically increases the maximum load, and that of H/L/C/T is about 1.3 times larger than that of H/L/C. The rate of load reduction after the maximum load becomes slow due to LTI addition, corresponding to the improvement of resistance against crack propagation.

Fracture properties calculated by Eqs. 1 and 2 are shown in Fig. 3b. HA/PLLA possesses lower fracture properties than pure PLLA, indicating that the dispersed HA particles tend to degrade these fracture properties. Blending of PCL to the composite can effectively improve the fracture properties and the fracture properties of H/L/C are nearly equal to those of PLLA. The fracture properties are dramatically improved by LTI addition; especially, E_f of H/L/C/T is about three times larger than that of H/L/C.

SEM micrographs of the mode I fracture surfaces in notch-tip region are shown in Fig. 4a–c. The fracture surface of H/L is characterized by a rough surface with void formation. These voids are thought to be created by debonding of HA particles from PLLA matrix. These voids likely cause local stress concentration in the surrounding regions, resulting in the accelerated crack initiation. The fracture surface of HA/L/C becomes rougher than that of H/L, corresponding to the enhancement of ductile deformation due to blending of ductile PCL phase. The amount of voids tends to increase by the PCL blending, and these voids are thought to be created by debonding of dispersed PCL spherulites from PLLA-rich phase [22]. These voids increase local stress concentration in the surrounding regions, while the ductile deformation of specimen increases, resulting in the slight improvement of G_{in} value. The amount of voids is dramatically reduced by LTI addition mainly owing to the improvement of miscibility of PLLA and PCL as shown in Fig. 2. It is noted that the amount of voids created by the debonding of HA particles is also effectively reduced due to LTI addition. FE-SEM micrographs of the interfacial structure between HA particles and PLLA/PCL matrix are shown in Fig. 5. It is considered that the interfacial connections between HA particles and PLLA/PCL matrix are effectively strengthened due to LTI addition, resulting in the reduction of void formation. These micro-structural changes of blend morphology and interfacial structure reduce the localized stress concentration regions and lead to the enhancement of ductile deformation and result in the increase of the G_{in} value.

SEM micrographs of the mode I fracture surfaces in crack propagation region that is distant from the notch-tip by about 1 mm are shown in Fig. 4d–f. The fracture surface of H/L is characterized by smooth surface, corresponding to the low fracture energy. The fracture surface of H/L/C is characterized by void formation and becomes rougher than that of H/L. The voids are thought to be mainly created by debonding of HA particles from the PLLA/PCL matrix. These voids generate local stress concentrations in the surrounding regions, resulting in the increase of local ductile deformation and the slight

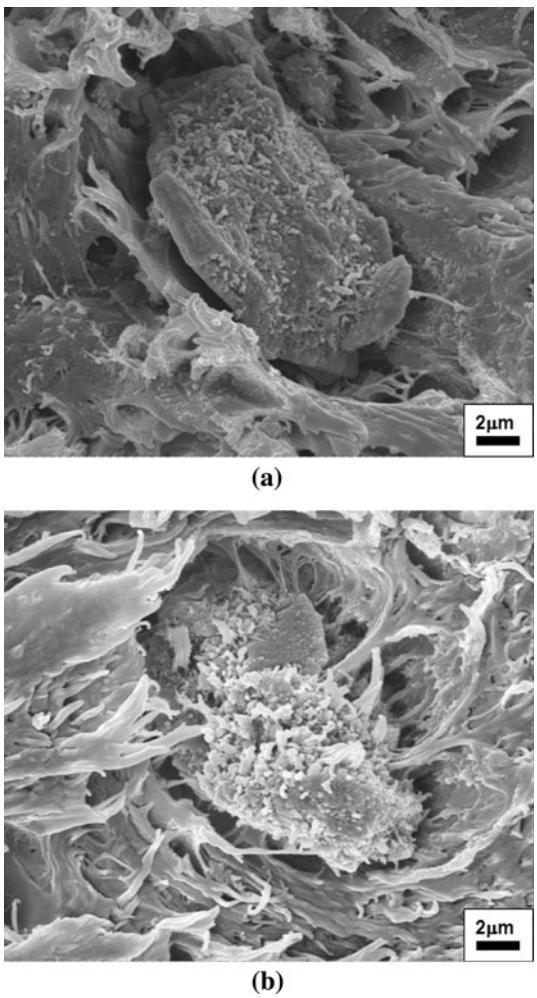

Fig. 5 FE-SEM micrographs of interfacial structure between HA particle and PLLA matrix. **a** HA/PLLA/PCL and **b** HA/PLLA/PCL/LTI

improvement of E_f value. The amount of voids is reduced dramatically due to LTI addition as a result of improvement of the interfacial connections between HA particles and PLLA/PCL matrix as shown in Fig. 5. These micro-structural changes of blend morphology and interfacial structure reduce the localized stress concentration regions and lead to the ductile deformation and resulted in the increase of E_f value.

In summary, effects of LTI addition on the mode I fracture properties of HA/PLLA/PCL were examined and the micro-structural modification due to LTI addition was investigated. Both the energy release rate at crack initiation and the average fracture energy are improved dramatically due to LTI addition. The reasons for such improvements are considered to be the strengthening of the interfacial connection between HA particles and PLLA/PCL matrix and the improvement of miscibility of PLLA and PCL. These changes of blend morphology and interfacial connection reduce the stress concentration and lead to the ductile deformation and resulted in the increase of those fracture properties.

References

1. Leenslag JW, Pennings AJ, Bos RRM, Rozema FR, Boering J (1987) Biomaterials 8:70
2. Bostman OM (1991) J Bone Joint Surg 73A:148
3. Shikinami Y, Okuno M (1999) Biomaterials 20:859
4. Yasunaga T, Matsusue Y, Furukawa T, Shikinami Y, Okuno M, Nakamura T (1999) J Biomed Mater Res 47:412
5. Kasuga T, Ota Y, Nogami M, Abe Y (2001) Biomaterials 22:19
6. Rizzi SC, Heath DJ, Coombes AGA, Bock N, Textor M, Downes S (1999) J Biomed Mater Res 47:475
7. Furukawa T, Matsusue Y, Yasunaga T, Nakagawa Y, Okada Y, Shikinami Y, Okuno M, Nakamura T (2000) J Biomed Mater Res 50:410
8. Furukawa T, Matsusue Y, Yasunaga T, Shikinami Y, Okuno M, Nakamura T (2000) Biomaterials 21:889
9. Deng X, Hao J, Wang C (2001) Biomaterials 22:2867
10. Shikinami Y, Matsusue Y, Nakamura T (2005) Biomaterials 26: 5542
11. Hong Z, Zhang P, He C, Qiu X, Liu A, Chen L, Chen X, Jing X (2005) Biomaterials 26:6296
12. Debra DWC, Julia AK, Darinda MM, Cho LM (2006) J Biomed Mater Res A 78A:541
13. Fang L, Yan J, Xiaodan L, Demin J (2006) J Appl Polym Sci 102:4085
14. Kikuchi M, Suetsugu Y, Tanaka J (1997) J Mater Sci Mater Med 8:361
15. Verheyen CCPM, de Wijn JR, van Blitterswijk CA, de Groot K (1992) J Biomed Mater Res 26:1277
16. Todo M, Park SD, Arakawa K, Takenoshita Y (2006) Composites A 37:2221
17. Park SD, Todo M, Arakawa K, Takenoshita Y (2005) Key Eng Mater 297–300:2453
18. Todo M, Kagawa T (2007) J Mater Sci 43:799. doi:10.1007/s10853-007-2308-0
19. Park SD, Todo M, Arakawa K, Tsuji H, Takenoshita Y (2005) Proc SPIE 5852:838
20. Takayama T, Todo M, Tsuji H, Arakawa K (2006) J Mater Sci 41:6501. doi:10.1007/s10853-006-0611-9
21. Takayama T, Todo M (2006) J Mater Sci 41:4989. doi:10.1007/s10853-006-0137-1
22. Takayama T, Todo M (2008) J Solid Mech Mater Eng 2:455
23. ASTM D 5041-91a. Standard test methods for plane-strain fracture toughness and strain energy release rate of plastic materials
24. Tsuji H, Yamada Y, Suzuki M, Itsuno S (2003) Polym Int 52:269